



# Preparation and Photocatalytic Activity of an Electrostatically Self-Assembled Film Made of $[\text{PMo}_{12}\text{O}_{40}]^{3-}$ and a Bipolar Hemicyanine Cation

Li-Hua Gao<sup>1,\*</sup>, Wen-Chan Jiang<sup>1</sup>, and Ke-Zhi Wang<sup>2</sup>

<sup>1</sup>Department of Chemistry, School of Science, Beijing Technology and Business University, Beijing 100048, China

<sup>2</sup>College of Chemistry, Beijing Normal University, Beijing 100875, China

An electrostatically self-assembled film of  $\text{PMo}_{12}/\text{H}^6$  has successfully been prepared on quartz substrates by alternating adsorption of  $[\text{PMo}_{12}\text{O}_{40}]^{3-}$  ( $\text{PMo}_{12}$ ) and a bipolar hemicyanine derivative of (*E*)-1,1'-(hexane-1,6-diyl)bis(4-(4-(dimethylamino)styryl)pyridinium) bromide ( $\text{H}^6\text{Br}_2$ ). The UV-visible spectra showed that the film was uniformly deposited and the charge transfer between two film-forming components might occur in the film. The photocatalytic performance of the film was studied for the degradation of aqueous dye Methyl Red (MR) under UV irradiation. The degradation of MR follows Langmuir-Hinshelwood first-order kinetics.

**Keywords:** Polyoxometalates, Hemicyanine, Self-Assembled Film, Photocatalysis, UV-Visible Spectroscopy.

Delivered by Publishing Technology to: Chinese University of Hong Kong

IP: 41.189.254.81 On: Mon, 07 Dec 2015 10:26:41

Copyright: American Scientific Publishers

## 1. INTRODUCTION

Since the photocatalytic degradation of inorganic and organic pollutants was introduced, the photocatalysts with high catalytic performance have attracted much attention because of their relation to solar energy conversion and environmental cleaning.<sup>1–3</sup> In recent years, there has been increasing interest in polyoxometalates (POMs), a class of inorganic metal-oxide clusters, for catalysis<sup>4</sup> and photocatalysis.<sup>5</sup> Although they have been used as an efficient photocatalyst for the removal of transition metal ions or organic pollutants from water,<sup>6</sup> which is analogous to  $\text{TiO}_2$ , a major drawback to the practical applications of the POM system is its high water solubility, which impedes recovery and reuse of the catalyst. To conquer this shortcoming, much work has been centered on the preparation of insoluble POM catalysts, such as support of POMs on high surface area solids such as zeolite,<sup>7</sup>  $\text{SiO}_2$ ,<sup>8</sup> and  $\text{TiO}_2$ ,<sup>9</sup> intercalation of POMs into layered double hydroxides,<sup>10</sup> and precipitation of POMs with large cations to form insoluble salts.<sup>11</sup> Recently, Hu et al. reported the composite films  $\text{POM}/\text{SiO}_2$  and  $\text{POM}/\text{TiO}_2$  prepared by the sol-gel method as well as the spin-coating technique for photocatalytic degradation of organic pollutants.<sup>12,13</sup> Undoubtedly, POM-containing films as catalysts have the advantage of easier handling for recycling

uses. Among the techniques for the fabrication of ultrathin films, the electrostatic self assembly pioneered by Decher<sup>14</sup> has proved to be one of the most attractive techniques, which could achieve multilayer assemblies by simple electrostatic attraction of oppositely charged species on a layer-by-layer (LBL) basis with precisely controlled thickness and layer sequences. To the best of our knowledge, no reports have been made on the photocatalytic application of POM-containing self-assembled films. Here, a bipolar hemicyanine derivative of (*E*)-1,1'-(hexane-1,6-diyl)bis(4-(4-(dimethylamino)styryl)pyridinium) bromide (hereafter abbreviated as  $\text{H}^6\text{Br}_2$ ) and a Keggin anion of  $[\text{PMo}_{12}\text{O}_{40}]^{3-}$  (hereafter abbreviated as  $\text{PMo}_{12}$ ) were selected for use in the fabrication of an electrostatically self-assembled film. The photocatalytic behavior of the film for degradation of aqueous MR under near-ultraviolet (UV) irradiation was studied.

## 2. EXPERIMENTAL DETAILS

### 2.1. Materials

3-Aminopropyltrimethoxysilane (98%) was purchased from Acros. Other chemicals were commercially available and were used without further purification.

$\text{PMo}_{12}$  was prepared according to the literature method.<sup>15</sup>  $\text{H}^6\text{Br}_2$  was synthesized by the route shown in Figure 1.

\* Author to whom correspondence should be addressed.

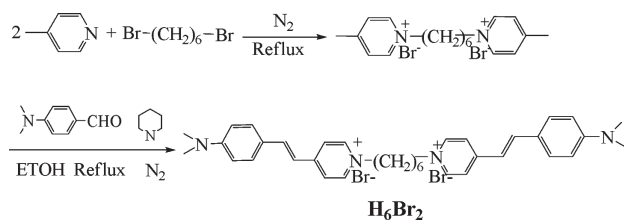


Fig. 1. Synthetic route to dipolar hemicyanine  $\text{H}^6\text{Br}_2$ .

First, 1,1'-(hexane-1,6-diyl)bis(4-methylpyridinium) bromide was prepared by the recrystallization of ethanol-ethyl ether powder which was made by refluxing 20 mmol of 1,6-dibromohexane with 40 mmol of 4-methylpyridine at 130 °C. Then 5 mmol of the obtained 1,1'-(hexane-1,6-diyl)bis(4-methylpyridinium) bromide was mixed with 10 mmol of 4-(*N,N*-dimethylamino)benzaldehyde and 1 mL of piperidine in 30 mL absolute ethanol and refluxed for 7 h. On cooling the reaction mixture to the room temperature, a red product formed, was filtered, and was recrystallized three times from ethanol, giving 2.6 g of  $\text{H}^6\text{Br}_2$  (76%). M. p. 282~283 °C. Anal. Calcd. for  $\text{C}_{36}\text{H}_{44}\text{N}_4\text{Br}_2$ : C, 62.43; H, 6.40; N, 8.09. Found: C, 62.30; H, 6.20; N, 8.00. IR (KBr,  $\text{cm}^{-1}$ ): 2996w, 2926w, 2860w, 1612w, 1586vs, 1528s, 1472w, 1452w, 1435w, 1365m, 1331m, 1211w, 1191w, 1167s, 1127w, 1068w, 1046w, 981w, 946w, 880w, 826w.  $^1\text{H}$  NMR (500 MHz,  $\text{DMSO}-d_6$ ):  $\delta$  ppm 8.80~8.81(4H, d,  $-\text{C}_5\text{H}_4\text{N}$ ), 8.08~8.09(4H, d,  $-\text{C}_5\text{H}_4\text{N}$ ), 7.93~7.96(2H, d,  $=\text{CH}-$ ), 7.60~7.61(4H, d,  $-\text{Ar}-\text{H}$ ), 7.18~7.21(2H, d,  $-\text{CH}=-$ ), 6.78~6.80(4H, d,  $-\text{Ar}-\text{H}$ ), 4.42~4.45(4H, t,  $\text{N}-\text{CH}_2$ ), 3.03(12H, s,  $-\text{N}(\text{CH}_3)_2$ ), 1.89(4H, s,  $\text{NCH}_2-\text{CH}_2$ ), 1.32(4H, s,  $\text{NCH}_2\text{CH}_2-\text{CH}_2$ ).

## 2.2. Film Preparation

The protonation of the 3-aminopropyltrimethoxysilaned quartz substrate was performed as described before.<sup>16</sup> The substrate was then immersed for 30 min in an aqueous solution of 1.0 mM  $\text{PMo}_{12}$  to adsorb a negatively charged  $\text{PMo}_{12}$  monolayer. After washing with water and drying with  $\text{N}_2$ , the  $\text{PMo}_{12}$ -coated substrate was placed for 30 min

in 1.0 mM  $\text{H}^6\text{Br}_2$  aqueous solution. Repetition of the above two steps yielded a  $(\text{PMo}_{12}/\text{H}^6)_n$  ( $n$  stands for the number of bilayers) multilayer as shown in Figure 2.

## 2.3. Physical Measurements

C, H, and N elemental analyses were performed on a Vario EL elemental analyzer. Infrared spectra were measured on a Nicolet Avatar 360 FT-IR (Fourier transform infrared) spectrometer as KBr disks. An  $^1\text{H}$  nuclear magnetic resonance (NMR) spectrum was obtained on a Bruker DRX-500 spectrometer. UV-visible (UV-vis) spectra were obtained on a GBC Cintra 10e UV-vis spectrophotometer.

## 2.4. Photocatalytic Procedure

An XPA-1 photoreactor made by Nanjing Xujiang Electromechanical Plant equipped with a water circulating jacket and an opening for supply of air was used throughout the experiment. The light source was a 300 W high-pressure mercury lamp. For irradiation experiments, 4 mL of MR solution (25  $\mu\text{M}$ ) and a slide of the film (1 cm  $\times$  2 cm) were placed into the photoreactor. All degradation experiments were carried out at room temperature with the photoreactor open to air. Decreases in the concentrations of MR were analyzed by UV-vis spectroscopy. At given intervals of illumination, a sample of reaction solution was taken out and the changes in absorbance at  $\lambda_{\text{max}}$  523 nm of a peak maximum for MR were measured.

## 3. RESULTS AND DISCUSSION

### 3.1. UV-Visible Absorption Characteristics of $(\text{PMo}_{12}/\text{H}^6)_n$ Films

UV-visible spectroscopy was used to monitor the process of fabricating the hybrid multilayer films of  $(\text{PMo}_{12}/\text{H}^6)_n$  on quartz substrates. Figure 3 shows the comparison of the absorption spectra for  $\text{PMo}_{12}$  in  $\text{H}_2\text{O}$ ,  $\text{H}^6\text{Br}_2$  in  $\text{H}_2\text{O}$ , and a 10-layer  $(\text{PMo}_{12}/\text{H}^6)_{10}$  film. It is clearly seen that the  $\text{PMo}_{12}$  aqueous solution exhibited a strong  $\text{O}_d \rightarrow \text{Mo}$

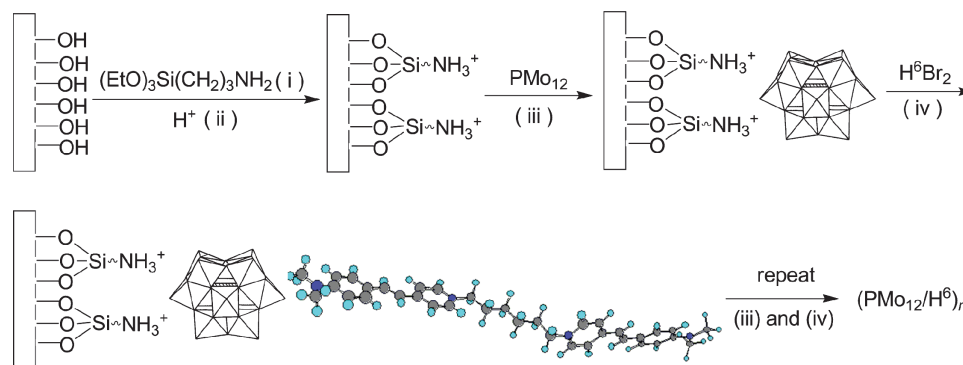
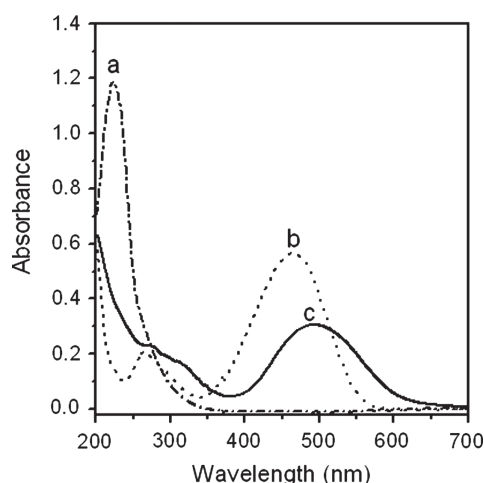


Fig. 2. Schematic illustration of the multilayer assembly of  $(\text{PMo}_{12}/\text{H}^6)_n$ .



**Fig. 3.** The comparison of absorption spectra for  $\text{PMo}_{12}$  in (a)  $\text{H}_2\text{O}$ , (b)  $\text{H}^6\text{Br}_2$  in  $\text{H}_2\text{O}$ , and (c)  $(\text{PMo}_{12}/\text{H}^6)_n$  film.

charge transfer (CT) absorption band at 220 nm. The  $\text{H}^6\text{Br}_2$  aqueous solution gave a  $\pi \rightarrow \pi^*$  absorption band at 265 nm and a CT absorption band at 459 nm,<sup>16</sup> the multilayer film of  $(\text{PMo}_{12}/\text{H}^6)_{10}$  exhibited two absorption bands at 275 and 492 nm. The former band was the superposition of the  $\text{PMo}_{12}$ -based and  $\text{H}^6\text{Br}_2$ -based CT absorption bands because the intensity of the absorption band at 275 nm is stronger than that of the absorption band at 492 nm. The latter band has a characteristic of  $\text{H}^6\text{Br}_2$ -based CT absorption and is red shifted by 33 nm compared with the  $\text{H}^6\text{Br}_2$ -based CT band for the aqueous solution. This indicates that  $\text{PMo}_{12}$  and  $\text{H}^6$  were successfully assembled into the film. The red-shift observed for the CT transition between the film and the solution is most probably due to the charge transfer between  $\text{PMo}_{12}$  and  $\text{H}^6\text{Br}_2$ , which has already been observed in previously reported hemicyanine-containing electrostatically LBL self-assembled films.<sup>17–19</sup>

Figure 4 shows the UV-vis absorption spectra of the LBL growth of the  $(\text{PMo}_{12}/\text{H}^6)_n$  self-assembled multilayer film on a quartz substrate. As shown in Figure 4, the absorption maxima are independent of the number of layers deposited, indicating that the interlayer molecular interaction is independent of layer number. The absorptions of the films at 492 nm increased linearly with the number of deposited  $(\text{PMo}_{12}/\text{H}^6)_n$  layers (inset of Fig. 4) with correlation coefficients of 0.9970, demonstrating that the film deposition is uniform and reproducible.

From the Lambert–Beer law of modification for two-dimensional concentration—i.e.,  $\Gamma = 10^{-3}D/\epsilon$ ,<sup>20</sup> where  $\Gamma$  is the surface concentration ( $\text{mol cm}^{-2}$ ),  $D$  is the absorbance per layer, and  $\epsilon$  is the molar extinction coefficient for the film-forming molecule in the film at a fixed wavelength—the absorbance per layer at 492 nm, calculated from the slope in the linear relationship in the inset of Figure 4, was found to be  $1.67 \times 10^{-2}$ . If we suppose that an  $\epsilon$  value at 492 nm for  $\text{H}^6\text{Br}_2$  in the films is

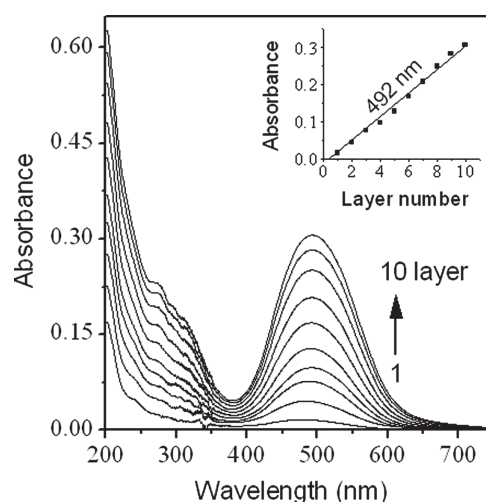


**Fig. 4.** The absorption spectra of  $(\text{PMo}_{12}/\text{H}^6)_n$  multilayers ( $n = 1$  to 10) on double sides of quartz. The inset is the plot of absorbance at 492 nm of the films versus layer number.

approximately equal to  $2.45 \times 10^4$  for  $\text{H}^6\text{Br}_2$  in aqueous solution, the surface concentration of  $\text{H}^6\text{Br}_2$  in the film is derived to be  $6.8 \times 10^{-10} \text{ mol cm}^{-2}$ . The occupied area per molecule is derived to be  $0.24 \text{ nm}^2$ .

### 3.2. Photocatalytic Activity

In order to study the photocatalytic activity of films, we chose azo-compound Methyl Red (Fig. 5)—a non-biodegradable organic pollutant and represents an increasing environmental danger—as the model pollutant. The results of degradation of aqueous MR under irradiation in the near-UV range are shown in Figure 6. When the film was put into the aqueous MR solution, and was placed in the dark for 220 min, MR was negligibly degraded. However, apparent decreases in the concentrations of MR were observed by irradiating the MR solutions in the presence of one slide of  $(\text{PMo}_{12}/\text{H}^6)_{14}/\text{PMo}_{12}$  film, i.e., degradation of MR was about 68% when irradiation time was 220 min. These results suggest that degradation of MR mainly originated from photocatalysis of the  $(\text{PMo}_{12}/\text{H}^6)_{14}/\text{PMo}_{12}$  film. The photocatalytic activity of the  $(\text{PMo}_{12}/\text{H}^6)_{14}/\text{PMo}_{12}$  film is attributed to  $\text{PMo}_{12}$  component, which shares photochemical characteristics similar to that of semiconductors such as  $\text{TiO}_2$ ,<sup>21</sup> that is, its highest occupied molecular orbital (HOMO) and lowest unoccupied molecular orbital (LUMO) resemble the valence and conduction bands of semiconductors, respectively. The charge transfer from  $\text{O}^{2-}$  to  $\text{Mo}^{6+}$  in the  $\text{PMo}_{12}$  occurs as a result of UV irradiation, resulting in the formation of a hole ( $\text{O}^-$ ) and a

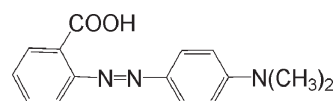


**Fig. 5.** Structure of MR.

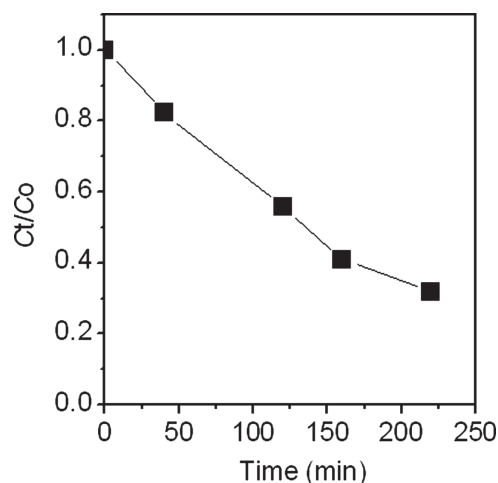


**Fig. 6.** Changes in MR concentrations as a function of UV irradiation time. Conditions:  $C_0 = 25 \mu\text{M}$ ,  $V_{\text{MR}} = 4 \text{ ml}$ .

trapped electron center ( $\text{Mo}^{5+}$ ), i.e., the charge-transfer excited state  $\text{PMo}_{12}^*$ .  $\text{O}^-$  has strong oxidation ability,<sup>22</sup> and is also responsible for the oxidation of the MR dye.

The degradation behavior of MR can be described by the Langmuir-Hinshelwood rate Eq. (1),<sup>23</sup> which is further simplified to be a pseudo-first-order rate Eq. (2) with respect to the MR concentration for experiments conducted with low concentrations of MR:

$$r = -\frac{dC}{dt} = \frac{kKC}{1+KC} \quad (1)$$

$$r = -\frac{dC}{dt} = k_{\text{app}}C \quad (2)$$

where  $C$  is the MR concentration in solution at illumination time  $t$ ,  $k$  is the rate constant,  $K$  is the equilibrium adsorption constant, and  $k_{\text{app}}$  is the apparent pseudo-first-order rate constant. Integrating Eq. (2) gives

$$\ln\left(\frac{C_0}{C_t}\right) = k_{\text{app}}t \quad (3)$$

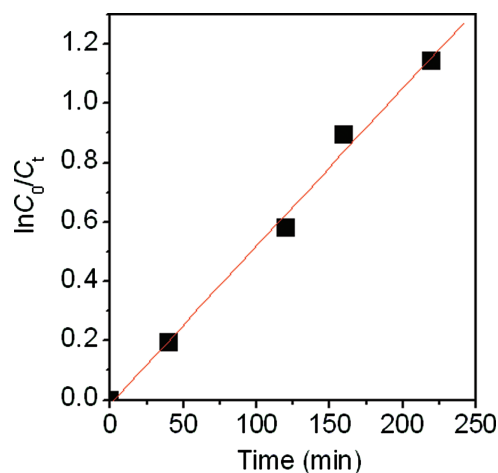


**Fig. 7.** First-order linear relation  $\ln(C_0/C_t) = k_{\text{app}}t$ . Conditions:  $C_0 = 25 \mu\text{M}$ ,  $V_{\text{MR}} = 4 \text{ ml}$ .

where  $C_0$  is the initial MR concentration in solution, and  $t$  is the illumination time. The results of MR degradation kinetics in aqueous solution under UV light irradiation are shown in Figure 7. It can be seen that a plot of  $\ln(C_0/C)$  versus  $t$  represents a straight line, indicating the MR degradations follow an apparent first order process. The apparent first-order rate constant  $k_{\text{app}}$  was derived to be  $0.0053 \text{ min}^{-1}$  by a slope of the linear regression.

## 4. CONCLUSIONS

We have successfully assembled an electrostatic self-assembled film by alternating adsorption of a Keggin anion of  $[\text{PMo}_{12}\text{O}_{40}]^{3-}$  and a bipolar hemicyanine derivative of (*E*)-1,1'-(hexane-1,6-diyl)bis(4-(4-(dimethylamino)styryl)pyridinium) bromide. The film exhibits interesting photocatalytic activity for the degradation of aqueous dye Methyl Red under UV irradiation. The degradation of MR follows Langmuir-Hinshelwood first-order kinetics. The results indicate that this film photocatalyst for recycling uses has the advantage of easy separation from the reaction system over powdered or soluble catalysts.

**Acknowledgments:** The authors thank the National Natural Science Foundation (Nos. 20971016, 90922004, 20871011, 21171022), Beijing Natural Science Foundation (2072011, 2092011), Funding Project for Innovation on Science, Technology and Graduate Education in Institutions of Higher Learning Under the Jurisdiction of Beijing Municipality and Measurements Fund of Beijing Normal University for financial support.

## References and Notes

1. D. Y. Goswami, *J. Solar Energy Eng.* 119, 101 (1997).
2. M. R. Hoffmann, S. T. Martin, W. Chio, and D. W. Bahnemann, *Chem. Rev.* 95, 69 (1995).
3. Y. H. Hsien, C. F. Chang, and Y. H. Chen, *Appl. Catal. B* 31, 241 (2001).
4. N. Mizuno and M. Misono, *Chem. Rev.* 98, 199 (1998).
5. A. Hiskia, A. Troupis, S. Antonaraki, E. Gkika, and E. Papaconstantinou, *Int. J. Environ. Anal. Chem.* 86, 233 (2006).
6. E. Gkika, A. Troupis, A. Hiskia, and E. Papaconstantinou, *Appl. Catal., B: Environmental* 62, 28 (2006).
7. R. R. Ozer and J. L. Ferry, *J. Phys. Chem. B* 106, 4336 (2002).
8. Y. H. Guo, Y. H. Wang, C. W. Hu, E. B. Wang, Y. C. Zhou, and S. H. Feng, *Chem. Mater.* 12, 3501 (2000).
9. C. C. Chen, P. X. Lei, H. W. Ji, W. H. Ma, J. C. Zhao, H. Hidaka, and N. Serpone, *Environ. Sci. Tech.* 38, 329 (2004).
10. Y. H. Guo, D. F. Li, C. W. Hu, Y. H. Wang, and E. B. Wang, *Int. J. Inorg. Mater.* 3, 347 (2001).
11. Z. W. Xi, N. Zhou, Y. Sun, and K. L. Li, *Science* 292, 1139 (2001).
12. D. F. Li, Y. H. Guo, C. W. Hu, L. Mao, and E. B. Wang, *Appl. Catal. A: General* 235, 11 (2002).
13. Y. Yang, Y. H. Guo, C. W. Hu, and E. B. Wang, *Appl. Catal. A: General* 252, 305 (2003).
14. G. Decher, *Science* 277, 1232 (1997).
15. H. Wu, *J. Biol. Chem.* 43, 189 (1920).

16. L. Y. Wang, K. Z. Wang, and L. H. Gao, *Acta Chim. Sinica* 61, 1877 (2003).
17. L. H. Gao, X. J. Hu, D. S. Zhang, Y. Guo, and K. Z. Wang, *J. Nanosci. Nanotechnol.* 8, 1355 (2008).
18. L. H. Gao, K. Z. Wang, and L. Y. Wang, *J. Nanosci. Nanotechnol.* 10, 2108 (2010).
19. L. H. Gao, L. Y. Wang, and K. Z. Wang, *Solid State Phenomena* 121–123, 457 (2007).
20. L. H. Gao, K. Z. Wang, L. Cai, H. X. Zhang, L. P. Jin, C. H. Huang, and H. J. Gao, *J. Phys. Chem. B.* 110, 7402 (2006).
21. A. Hiskia, A. Mylonas, and E. Papaconstantinou, *Chem. Soc. Rev.* 30, 62 (2001).
22. Y. Yang, Y. H. Guo, C. W. Hu, Y. H. Wang, and E. B. Wang, *Appl. Catal. A: General* 273, 201 (2004).
23. Y. Ku, W. H. Lee, and W. Y. Wang, *J. Mol. Catal. A: Chem.* 273, 191 (2004).

Received: 13 November 2010. Accepted: 18 April 2011.

Delivered by Publishing Technology to: Chinese University of Hong Kong  
IP: 41.189.254.81 On: Mon, 07 Dec 2015 10:26:41  
Copyright: American Scientific Publishers

RESEARCH ARTICLE